SOY PROTEIN FILM REINFORCED WITH SILVER NANOPARTICLE ANCHORED CARBON DOTS AND CHITIN NANOWHISKER FOR PACKAGING

Dissertation submitted in partial fulfillment of the requirement for the award of degree of Master of Science in Analytical Chemistry, Kerala University Trivandrum, Kerala

JUNE 2022

EXAM CODE : 63620401

COURSE CODE : CL 243

ABSTRACT

This study demonstrates a great strategy for developing active biopolymer film from soy protein isolate (SPI) with silver nanoparticles anchored carbon dots and chitin nanowhiskher. In this work, we have adopted an environment-friendly method where carbon dot (CD) prepared from soy protein isolate is used to prepare AgNPs. AgNP (1% wt.) and different concentrations of chitin nanowhisker (CNW) (2-10% wt.) were added to soy protein isolate to fabricate nanocomposite films. The prepared SPI based bionanocomposite films were characterized by FTIR, XRD and SEM. Commercial production of such SPI films would revolutionize the food packaging industry given its health benefits and cost effectiveness.

CONTENTS

Page No.

LIST OF FIGURES

LIST OF ABBREVATIONS

SPI	**Soy Protein Isolate**
FTIR	**Fourier Transform Infrared Spectroscopy**
TEM	**Transmission Electron Microscopy**
SEM	**Scanning Electron Microscopy**
CNW	**Chitin Nano Whiskher**
AgNP	**Silver Nano Particles**
CHW	**Chitin Whiskher**
CD	**Carbon dot**
XRD	**Xray diffractometer**
WVP	**Water Vapour Permiability**
Nm	**Nanometre**

CHAPTER 1

INTRODUCTION

Hectic modern-day lifestyle, coupled with a growing need for consumption of fresh-cut vegetables, fruits and cooked food on the go, has generated the pressing need for safe packaging material. However, the safety and quality of such packaging material is always a matter of suspect with the food materials thus packed being generally susceptible to bacterial and microbial contamination[1]. Contamination by pathogens such as *Escherichia coli, Staphylococcus aureus, Listeria monocytogenes and Aspergillus niger* can cause gastric health problems and even death[2]. Hence new techniques are being used to increase the shelf-life of the food items, the most important among them being the use of antibacterial biopolymer coating and packaging films[3].

In recent decades there has been speedily growing interests in developing intelligent packaging films as freshness sensors[4], which is a very important side for recent, top quality and safe foods. Development in food packaging with the conception of incorporating active compounds into packaging materials or its encompassing conditions that is referred to as 'active packaging' evolved recently. Of late, the area of active and intelligent packing has gained popularity among researchers. Intelligent packaging interacts deliberately with the product in order to improve food quality and safety. Thus, active and intelligent packaging extends the protection and information functions of traditional packaging. Intelligent packaging is a system capable of monitoring food conditions in real time, enhancing possibilities to monitor product quality, trace critical points, and give more detailed information throughout the supply chain. The information is communicated through direct visual changes[5]. The intelligent packaging system can be used as a sachet, attached as labels or tags, incorporated into, or printed onto packaging material. This technology is thus a system with advantages of providing the user with ability to monitor and record the critical parameters for the food quality such as changes in the food, its environment condition, and packaging integrity[6]. This development has led to an efficient and consistent food supply chain, causing a decrease in food loss and wastage.

One third (about 1.3 billion tons) of food produced for human consumption is lost or wasted in the food supply chain every year. Focusing on developed countries, more than 40% of food losses happen at retail and consumer levels, due to legal requirements regarding food quality or safety, as well as consumers' expectations and decision-making criteria (FAO, 2015). Current date labels like 'Best Before' may not be able to provide consumers with real-time information about food freshness, safety, and quality, it is evident that there is a pressing need to replace or modify food date labels for more accurate food control. In addition to the sustainability of food packaging, accurate information of shelf

life is another major problem to be addressed [7]. The remaining shelf life of products cannot be simply judged through “expiration date” on the package, since it might be affected by various factors such as mishandling, abused temperature, etc. To obtain the precise quality information of the products, all the decisive elements must be taken into consideration. Intelligent food packaging is attracting great attentions from both industry and academia for monitoring storage conditions of the packed food, thereby precisely evaluating the real-time quality of the products[8,9].

Compared to synthetic polymers, the use of biopolymer-based packaging has grown and several biopolymeric matrices are available for biodegradable packaging[10]. Soy protein, a byproduct of soybean oil production, is one such matrix. Soy protein, based on its protein content, is classified as soy flour, soy protein concentrate and soy protein isolate. Soy protein isolate [SPI] containing 90% protein is the most commonly used form for film formation. However, due to its inherent hydrophilicity, soy protein by itself cannot produce good polymeric films. Hence, nanofillers, both organic and inorganic are added to the SPI matrix. Chitin nanowhisker (CNW) isolated from chitin is a filler commonly used in biopolymeric matrices due to its natural abundance, low cost, high aspect ratio, biodegradability, non-toxicity, crystallinity etc. Chitin is the second most abundant polymer found in the exoskeleton of crabs, shrimps, prawns and insects, and the cell walls of yeast, fungi and mushrooms. CNW is extracted from chitin using methods such as acid hydrolysis and TEMPO-oxidation[11]. However, all the reported methods are time-consuming and require several days. Though the reinforcing effect of CNW on biopolymer films such as starch carboxymethyl, cellulose, gelatin, etc. has been widely reported, not much work has been done to study the effect of the addition of CNW on SPI matrix.

Silver nanoparticle (AgNP) is an inorganic antibacterial agent commonly added to biopolymeric matrices to enhance the antibacterial property and thermal stability. Moreover, the antibacterial property of AgNP is found to be significantly affected by its shape, size and also the method through which it is synthesized. Hence, a variety of synthetic routes have been envisaged to synthesize AgNP with better antibacterial properties[12]. However, commonly reported synthetic procedures are either high energy-consuming or employ strong reducing agents leading to an uncontrollable reduction process. Meanwhile, in the absence of good stabilizing agents, the formed nanoparticles tend to easily aggregate leading to a reduction in antibacterial properties. Synthesizing AgNP using the reducing property of carbon dot (CD) particle is one good method to synthesize stable AgNP without the need for an extra stabilizing agent.

The AgNP gets anchored on the CD surface and the numerous OH and COOH groups on the surface of CD bind with Ag^+ and stabilize AgNP[13]

1.1 Nano Particles

Nanotechnology is science, engineering and technology conducted at the nanoscale which is about 1-100 nm. Physicist Richard Feynman is regarded as the father of nanotechnology. It is one of the most emerging field in 21st century. 'Nanotech' products that are on the market today are mostly gradually improved products where some form of nano-enabled material (such as carbon nanotubes ,nanocomposite structures or nanoparticles of a particular substance) or nanotech processes (eg: nano-patterning or quantum dots for medical imaging) is used in manufacturing process[14]. Nanoparticles can be made of materials of diverse chemical nature, the most common being metals, metal oxides, silicates, non-oxide ceramics, polymers, organics, carbon and biomolecules. Nanoparticles exist in several different morphologies such as spheres, cylinders, platelets, tubes etc. generally the nanoparticles are designed with surface modifications tailored to meet the needs of specific applications they are going to be used for. The enormous diversity of nanoparticles arising from their wide chemical nature, shape and morphologies, the medium in which these particles are present. The state of dispersion of the particles and the most importantly, the numerous possible surface modifications the nanoparticles can be subjected to make this an important active field of science now-a-days.

1.2 SOY PROTEIN

Figure 1 : Soy protein

Soy protein is a protein that is isolated from soyabean. Soyabean belongs to the family of Leguminosae genus Glysine L . It is the source of high-quality protein. Soyabean is made approximately of 38%

protein ,18% oil ,30% carbohydrate and 14% ash and moisture. In addition, they also contain mineral such as iron, copper, magnesium, calcium, zinc, cobalt, potassium, vitamins, and other minor components such as protease inhibitors, phenolic compounds and lictin. Soy protein polymers are macromolecules that contain a large number of amino acids and side chains that can be made use in the manufacture of plastics[15]. Plastics from SPI have high strength and good biodegradability. However, they are also brittle and water sensitive which limits their applications. The protein content of soy protein isolate (SPI) is more than those of other soy protein products, which make it hold a higher film-forming ability. Moreover, SPI –based films are clearer, smoother, and more flexible compared to other plant protein- based films, and they have impressive gas barrier properties compared with those films prepared from lipids and polysaccharides. SPI films possess excellent oxygen and lipid barrier properties. However, SPI individually do not show satisfactory physical, chemical, and mechanical properties for industrial applications. So, SPI has been blended with different plasticizers/matrices/fillers to achieve the desired properties[16]. Soy protein is the major component of soy- bean, and is readily available from renewable resources and agricultural processing by products. It is made from soybean meal that is defatted. It is a storage protein held in discrete particles called protein bodies which are estimated to contain at least 60-70% total soybean protein. The utilization of soy protein in the preparation of biodegradable materials, such as adhesives, plastics and various binders, has received more attention in recent years. Soy protein isolate is a highly refined or purified form of soy protein with a protein content of 90% on a moisture free basis. It is made from defatted soy flour which has the most of the non- protein components, fats and carbohydrates removed. Because of this, it has neutral flavor and will cause less flatulence due to bacterial fermentation. SPI are used to improve the texture of meat products, increase protein content, to enhance moisture retention and are used as emulsifiers[17].

Soy protein polymers are macromolecules that contain a large number of amino acids and side chains that can be made use in the manufacture of plastics. Plastics from SPI have high strength and good biodegradability. However, they are also brittle and water sensitive which limits their applications. The protein content of soy protein isolate (SPI) is more than those of other soy protein products, which make it hold a higher film- forming ability. Moreover, SPI –based films are clearer, smoother, and more flexible compared to other plant protein- based films, and they have impressive gas barrier properties compared with those films prepared from lipids and polysaccharides. SPI films possess excellent oxygen and lipid barrier properties[18]. However, SPI individually do not show satisfactory physical, chemical,

and mechanical properties for industrial applications. So, SPI has been blended with different plasticizers/matrices/fillers to achieve the desired properties[19].

1.3 Silver Nano Particles

Silver nanoparticles are nanoparticles of silver of between 1 nm and 100 nm in size. While frequently described as being 'silver' some are composed of a large percentage of silver oxide due to their large ratio of surface to bulk silver atoms. Numerous shapes of nanoparticles can be constructed depending on the application at hand. Commonly used silver nanoparticles are spherical, but diamond, octagonal, and thin sheets are also common. Silver nanoparticles (AgNPs) are one of the most vital and fascinating nano materials among several metallic nanoparticles that are involved in biomedical applications[20]. AgNPs play an important role in nanoscience and nanotechnology, particularly in nanomedicine. They have multifunctional bio-applications for example, as antibacterial, antifungal, antiviral, anti-inflammatory, anti-angiogenic, and anti-cancer agents. The biological activity of AgNPs depends on the morphology and structure of AgNPs, controlled by size and shape of the particles . As far as size and shape are concerned, smaller size and truncated-triangular nanoparticles seem to be more effective and have superior properties. Although many studies successfully synthesized AgNPs with different shape and size ranges.

Figure 2: Silver nanoparticles

AgNPs seem to be alternative antibacterial agents to antibiotics and have the ability to overcome the bacterial resistance against antibiotics. Therefore, it is necessary to develop AgNPs as antibacterial agents. Among the several promising nanomaterials, AgNPs seem to be potential antibacterial agents due to their large surface-to-volume ratios and crystallographic surface structure.

1.4 Chitin Nano Whisker

Chitin is the second most abundant semi crystalline polysaccharide. Like cellulose, the amorphous domains of chitin can also be removed under certain conditions such as acidolysis to give rise to crystallites in nanoscale, which are the so-called chitin nanocrystals or chitin whiskers (CHWs). CHW together with other organic nanoparticles such as cellulose whisker (CW) and starch nanocrystal show many advantages over traditional inorganic nanoparticles such as easy availability, nontoxicity, biodegradability, low density, and easy modification. They have been widely used as substitutes for inorganic nanoparticles in reinforcing polymer nanocomposites[21]. The research and development of CHW related areas are much slower than those of CW. However, CHWs are still of strategic importance in the resource scarcity periods because of their abundant availability and special properties. During the past decade, increasing studies have been done on preparation of CHWs and their application in reinforcing polymer nanocomposites

1.5 Carbon dots.

Carbon dots are zero dimensional carbon based materials within the size range of a couple of tens of nanometers and can be adopted with N,S,P and B heteroatoms.They arechemically modifiable to upgrade and render a few extra useful properties. More recently,carbon dots have attracted numerous attentions. They were fluorescent carbon nanomaterial with a few one of a kind properties, including tunable emission great biocompatibility, fabulous optical properties including prolonging stability and resistance to photobleaching[22], good water solubility, ease of functionalization, low environmental hazard, lower cost and easy preparation. Thus, CDs have drawn considerable attention in bioimaging[23] drug delivery[24] , photocatalysis[25] , fluorescent sensing, electrochemical application[26], waste water treatment[27] , optical devices such as light-emitting devices[28]

Nowadays, researchers are focusing on the synthesis of CDs because of their superior properties and wide applications of CDs. In particular, much significant research efforts have been put forward especially on the doping of CDs with heteroatoms such as nitrogen and sulfur. Among them, nitrogen doping can significantly enhance the properties of the CDs and expand significantly enhance the properties of the CDs and expand their novel applications in various fields. Nowadays, researchers are focusing on the synthesis of CDs because of their superior properties and wide applications of CDs. In particular, much significant research efforts have been put forward especially on the doping of CDs with heteroatoms such as nitrogen and sulfur. Different approaches have been established for the preparation

of CDs: top-down and bottom-up routes. Condensation and carbonization are performed from the bottom up and use different carbon precursors. In the top-down approach, the powerful techniques start with large pieces of graphite and generate CDs from them. Both approaches have inherent advantages.

The prepared C-dots show the chemical composition of nitrogen, hydrogen, and oxygen and other basic elements with respect to the substrate of preparation. Synthesis of C-dots is made possible in multiple ways including arc discharge[29], laser ablation[30], electrochemical[31], hydrothermal[32]l, ultrasonic, chemical oxidation[33], and microwave method[34]. Microwave-assisted technique, seems to be the most facile, time-saving and economical method and has been widely applied in virtue of simultaneous, homogeneous and efficient heating, which leads to fast reaction rate and uniform size distribution of products.

Hydrothermal synthesis is the best among them, forming high quantum yield C-dots with the advances in controlling the size, composition, purity, energy and cost-effectiveness. The instrument used for the fabrication of carbon dot by hydrothermal method is hydrothermal autoclave reactor in which synthesis is carried out at high pressure and high temperature. Hydrothermal method is one of the most common method for the synthesis of soy protein based carbon dots. Water is the common solvent used for the soy protein based carbon dot synthesis. Reaction temperature, reaction time and concentration of soy protein solutions are the important parameters that regulate the synthesis of carbon dots with quantum yield and good photoluminescence intensity.

The CDs showed the advantages of good biocompatibility, high photoluminescence and eco-friendly, and were widely used for sensors, fluorescent ink, hydro gel, bio imaging and drug delivery. Both man-made materials and natural products can be the carbon source of CDs. The preparation of fluorescent CDs without utilize organic chemicals (renewable resources) is called the green chemistry approach.the natural product and biomass subsidiaries are utilizes as a precursor for the green approaches of synthesis of CDs not as due to their abundance, non-toxicity, low cost but too green resource assisted strategy produces cd without any post – treatment. Since carbon is the element that can be found in every organic matter, CDs can be prepared from easily available organic matters. Starch, which widely exists in plants, is a readily accessible, low-cost, renewable and environmentally friendly raw material.

1.5.1 Application of Carbon Dots

- Carbon dots in cellular imaging: In recent years, CDs have been used as biosensors for detection of trace target biomolecules in various biological samples. CDs have been used as a new class of universal fluorescent probe to develop an optical biosensor for recognizing and detecting specific biomolecules.[35]
- Application of Carbon dots as efficient catalysis: Carbon materials have been used for a long time in heterogeneous catalysis, which can satisfy most of the desirable properties requested for suitable catalyst support. Based on their significant advantages, such as low cost, huge amount, easy accessibility, high surface area, diverse porous structure and resistance to acidic or basic environments, the carbon nanostructure are hungered for using as proper catalysts directly. Carbon dots, a new class of Carbon nanomaterials with size below 10nm, were also demonstrated to be efficient catalysts such as photocatalysis for selective oxidation, light-driven acid catalysis and hydrogen bond catalysis.
- Carbon dots used in Drug Delivery: Nanoparticles mainly including Carbon dots have been used in drug delivery systems to improve drug solubility, increase drug half-life and improve drug accumulation at the cancerous site. Therefore, this nanotechnology is a promising route for cellular imaging and drug delivery. Most of the dual nanodrug delivery systems fail to enter malignant brain tumorous due to a lack of proper targeting systems and the size increases of the nanoparticles after drug conjugation, therefore a triple conjugated system was developed with carbon dots, which have an average particle size of 1.5 -1.7 nm. CDs, where conjugated with transferrin and two anti-cancer drugs, epirubicin and temozolomide, to build the triple conjugated system, in which an average particle size was increased only upto 3.5nm
- A composite of self-passivated amorphous carbon dots (CDs) utilized to form fluorescent ink. The ink is invisible under visible light but glows brightly under external excitation. Cross-linking between the numerous surface groups present in the highly disordered CDs and chitin, endow the inks with enhanced optical and mechanical properties. The amorphous CD based ink is capable of writing on nearly all types of surfaces and exhibits excellent anti-clogging and anti-smearing properties. The luminescence yield, ultimate tensile were found to scale similarly with the concentration of CDs in chitin. All the parameters initially improve some optimal CD loading due to agglomeration effect.[36]

CHAPTER 2

REVIEW OF LITERATURE

- L Fang et al[37], in their work" Soy flour-derived carbon dots: facile preparation, fluorescence enhancement, and sensitive Fe^{3+} detection" they developed Soy flour-derived carbon quantum dots (C-dots) via a facile one-step hydrothermal approach. The as-prepared C-dots exhibit an average diameter of 2.5 nm and the crystalline lattices are consistent with graphitic carbons. Meanwhile, they show strong photoluminescence (quantum yield is 7.85 %), good water solubility, and high photostability. Importantly, structural defects of the C-dots were designed to obtain controllable fluorescence, which was achieved by changing the contents of N defects and O defects of C-dots. Their result shows that N defects can more effectively enhance the fluorescence emission than O defects. As the preparation temperature increases, the N defects are fine-tuned by substituting for partial O defects, reducing nonradiative recombination and enhancing fluorescence intensity, which is further confirmed by surface passivation.
- J Jana et al[38], in their work "Silver nanoparticle anchored carbon dots for improved sensing, catalytic and intriguing antimicrobial activity" they developed fluorescent carbon dots (NSCDs) with a size of ~5 nm (λex = 320 nm and λem = 386 nm) under reflux from an alkaline mixture of dopamine and cysteine. The synthesized NSCDs are hybridized with in situ generated silver nanoparticles (AgNPs) obtained by mixing AgNO3 at room temperature. NSCDs enrich the plasmonic bands of AgNPs due to the localized surface plasmon resonance (LSPR) effect. Their result shows that silver nanoparticle anchored carbon dots have a antimicrobial activity.
- X Zhai et al[39], in their work" Novel colorimetric films based on starch/polyvinyl alcohol incorporated with roselle anthocyanins for fish freshness monitoring" they developed Novel colorimetric films for real-time monitoring of fish freshness based on starch/polyvinyl alcohol (SPVA) incorporated with roselle (Hibiseus sabdariffa L.) anthocyanins (RACNs). Firstly, RACNs were extracted from roselle dehydrated calyxes. Secondly, SPVA aqueous solution was obtained with a mass rate of 2:1 (starch/PVA). Thirdly, the colorimetric films were fabricated by immobilizing 30, 60 and 120 mg RACNs/100 g starch into SPVA matrix with casting/solvent evaporation method. Their result shows that the colorimetric films presented visible color changes over time due to a variety of basic volatile amines.so these colorimetric films can be used to monitor the real-time fish freshness for intelligent packaging.
- R.Aurlina et al[40], in their work "Antibacterial study of silver nanoparticles synthesized using Strychnos potatorum(linn) – Green synthesis method" they used bottom-up approach of nanoparticle production by green synthesis method is ecologically friendly, where the reaction is

catalyzed by Phyto molecules. This process is viewed as less harmful and alternative to more extensive physical and chemical treatments. Their work describes simple, fast, and eco-friendly approach for the production of silver nanoparticles (AgNPs) using Strychnos potatorum(linn) seed extract. Their result shows that, Antibacterial activity against Staphylococcus aureus, Klebsiella pneumonia and Escherichia coli were studied and the maximum inhibition zone is reported.

- S Rani et al[41], in their work "Functionalized carbon dot nanoparticles reinforced soy protein isolate biopolymeric film" they developed Amine and carboxyl functionalized carbon dots (CDs), i.e., citric acid polyethylenimine (CPI) and citric acid glycine (CCG) at different contents (0.05 to 0.5% w/w with respect to soy protein isolate (SPI)) were incorporated in glycerol plasticized SPI to produce CDs reinforced SPI films. Their results shows that the work will be helpful in fabricating functionalized CDs reinforced SPI film from the renewable resources with low water uptake and good mechanical properties.
- Rakesh Kumar et al[42], in their work "Material properties of ZnS nanoparticles incorporated soy protein isolate biopolymeric film" developed Glycerol plasticised soy protein isolate (SPI) films at different contents (1 to 5% w/w w.r.t SPI) of zinc sulphide (ZnS) nanoparticles were fabricated. SPI films and ZnS nanoparticles incorporated SPI films were structurally and mechanically characterised by Fourier transform infrared spectroscopy (FT-IR) and mechanical properties, respectively. Transmittance and water uptake studies were also carried out for ZnS nanoparticles incorporated SPI films. The results from transmittance, water uptake and FT-IR studies indicated a good compatibility between the ZnS nanoparticles and the SPI. TheIR results showed the absence of antibacterial effect in ZnS nanoparticles incorporated SPI film.
- S Rani et al[43], in their work "Preparation, Characterization and Antibacterial Evaluation of Soy Protein Isolate Biopolymeric Films Loaded with Nalidixic Acid" developed glycerol plasticized soy protein isolate (SPI) films at different contents (1 to 5% w/w w.r.t SPI) of nalidixic acid (NA) were fabricated by solution casting method. SPI films and NA incorporated SPI films were structurally and mechanically characterized by Fourier transform infrared spectroscopy (FTIR) and mechanical properties, respectively. Thermomechanical and water uptake studies were also carried out for NA incorporated SPI films. Antibacterial activity of NA incorporated SPI films against E. coli and L. monocytogenes were studied. The antibacterial studies of NA incorporated SPI film showed the clear zone of inhibition against both the

bacteria. Their results shows that this work will be helpful in fabricating NA incorporated SPI film from the renewable resources with significant antibacterial properties and reasonable mechanical properties.

- Tao Liu et al[44], in their work "An ultrastrong bioinspired soy protein isolate-based nanocomposite with graphene oxide intercalation" developed intercalating graphene oxide nanosheets into the SPI-glycerin matrix with a vacuum evaporation self-assembly technology. The obtained SPI-Glycerin grapheme oxide nanocomposite has shown enhanced tensile strength and modulus, due to the hierarchical layered structures, and increased hydrogen bonds and covalent amido bonds.
- Yoshida et al[45], in their work "Chitosan bio-based and intelligent films: Monitoring pH variations" developed and characterize the fast pH-colorimetric indicator device, applying a simple manufacturing technique, using food grade and biodegradable materials. The intelligent film was based on natural compounds as chitosan and anthocyanin (pH-colorimetric indicator). Chitosan intelligent films (C-ATH, 2.0 g/100 g) were obtained incorporating anthocyanin (1.0 g/100 g) in matrix films. The advantages of this system were the simple manufacturing process, biodegradability and usage of natural and safe compounds.
- Y Yan et al[46], in their work "Fabrication of homogeneous and enhanced soybean protein isolate-based composite films via incorporating TEMPO oxidized nanofibrillated cellulose stabilized nano-ZnO hybrid" developed different SPI-based composite films were prepared by incorporating nano-ZnO and 2,2,6,6-Tetramethylpiperidine 1-oxyl (TEMPO) oxidized nanofibrillated cellulose (TNFC) separately or together. Nano-ZnO was introduced to endow the films with multifunction capability, while TNFC was introduced to stabilize the nanoparticles. Both the macro-optical characterization and micro scanning electron microscope with energy dispersive X-ray (SEM-EDX) analysis indicated that TNFC could significantly decrease nano-ZnO aggregation and improve its dispersibility in the SPI matrix due to the mechanical restriction and physical adsorption effect of TNFC to the nano-ZnO. In addition to the improved dispersibility, incorporating nano-ZnO and TNFC benefitted the mechanical properties and thermo stability of the SPI-based composite films. Their work provides a valuable reference for nanoparticles dispersion and application in regards to polymer enhancement and multi-functionalization.

CHAPTER 3

OBJECTIVES

The main objectives of the work were to

- To synthesize carbon dot from soy protein isolate
- To synthesize of silver nano particle from SPI carbon dot
- To synthesize chitin nanowhisker from prawn shell
- Characterization of the nano particles
- To develop biofilms using SPI reinforced with silver nano particles anchored with carbon dot and chitin nano whisker
- FTIR analysis of the film
- SEM analysis of the film
- XRD analysis of the film
- To analyze the water vapour permeability of the film
- To analyze the biodegradability of the film

CHAPTER 4

MATERIALS AND METHODS

4.1 Materials

- Dried chitin shrimp shell flakes (Poly-(1-4)-β-N-acetyl-D-glucosamine)
- Soy protein isolate
- $AgNO_3$
- Glycerol
- Distilled water

4.2 Method

4.2.1 Preparation of SPI Carbon Dot

2.5 g of SPI in 20 mL water was heated in a hydrothermal autoclave at 180 ºC for 6 h. After cooling the autoclave, the resulting brown solution was centrifuged at a high speed (10,000 rpm) for 15 minutes, followed by the filtration of the upper brown solution using a 0.22 µm filter membrane. The solution was then dried and diluted with 50 mL water and stored at 4 ºC.

Soy protein → Hydrothermal process → Carbon dot

Figure 3: Schematic representation of synthesis of carbon dot

4.2.2 Preparation of AgNP- anchored carbon dot

2 mL of $AgNO_3$ solution was taken from 15 mM stock solution and added to 6 mL of CD solution and mixed thoroughly. The mixture was then placed in a UV chamber (365 nm) for 5 minutes. The solution

immediately turned to light brown, indicating the hybridization of AgNPs. This hybridized particle was labelled as AgNP. The resulting solution was centrifuged, freeze-dried to obtain a solid mass, which could be easily dispersed in water when needed . The anchoring is schematically given in figure 4.

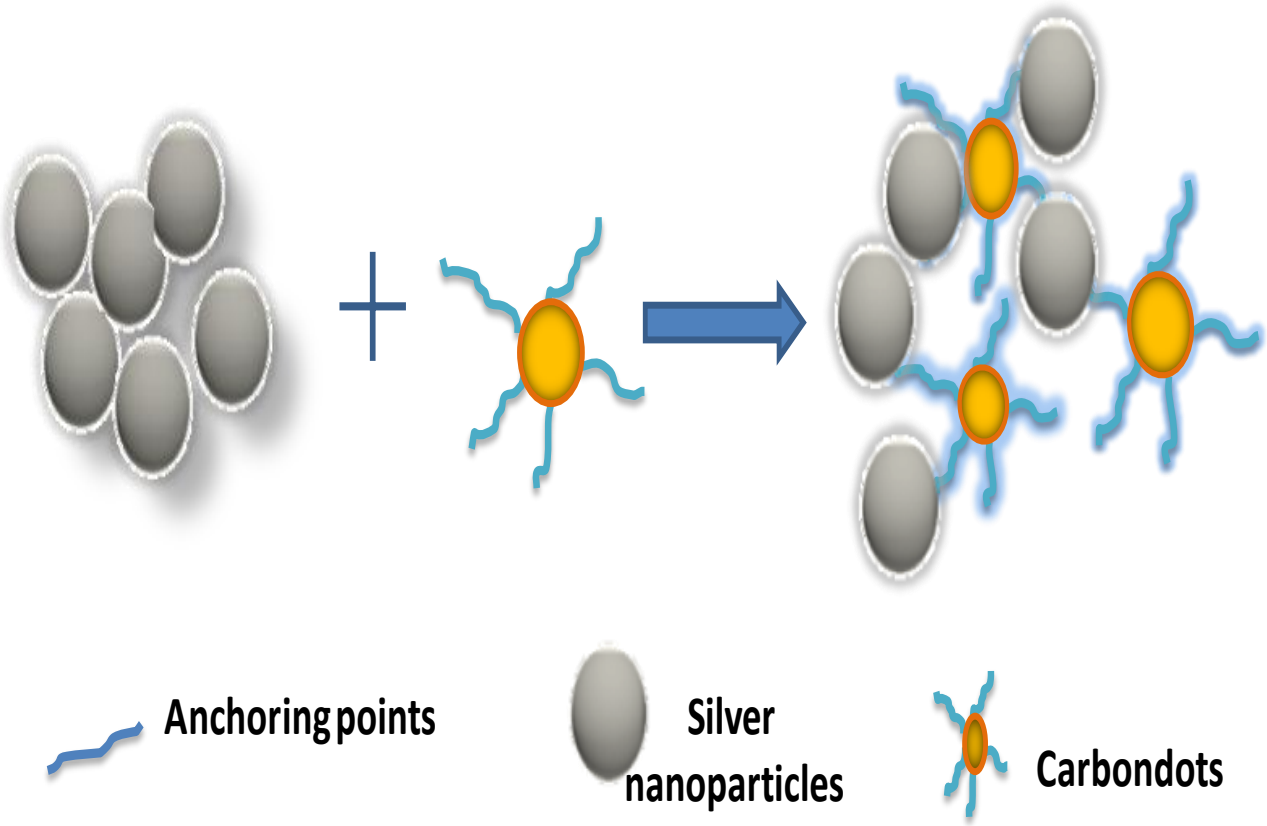

Figure 4. The possible interaction between the synthesized carbon dots and silver nanoparticles

4.2.3 Preparation of Chitin nanowhisker (CNW)

The procedures reported [47] to date for the isolation of CNW from raw chitin are tedious, take several days for completion and use an acidic medium to prevent agglomeration. Hence, we have adopted a new technique [IN patent 329388] for the isolation of CNW; using this, highly crystalline CNW can be extracted from raw chitin within a day under neutral conditions. This method involves the application of steam explosion technique using an autoclave for the extraction of CNW and involves three steps; deproteinization, demineralization and bleaching. In the deproteinization step, 40 gm of raw chitin flakes were treated with 3N NaOH under pressure in an autoclave for 30 minutes to remove the protein. After

washing the resulting suspension, demineralization was carried out wherein it was treated with 2N HCl in the same autoclave for half an hour. After releasing the pressure immediately and washing the suspension to neutral pH, bleaching was done using sodium chlorite water mixture (1:3). After bleaching, the suspension was thoroughly washed with distilled water and sonicated , to facilitate whisker formation.

4.2.4 Preparation of SPI/CNW-AgNP composite films

To prepare SPI film solution, 6 g of SPI powder was dissolved in 100 mL distilled water and 45 % (w/w of SPI) of glycerol was added as the plasticizer. The solution was heated at 80 ºC for 30 minutes. The film-forming solution was poured onto a Teflon-coated pan and dried in a vacuum oven overnight. For the preparation of SPI-CNW composite films, different concentrations of CNW (2%, 4%, 6%, 8%, 10% (w/w) of dry weight of SPI) were added to the film-forming SPI solution and stirred at a temperature of 60 ºC for half an hour [48]. The film-forming solutions were poured onto a Teflon plate (diameter 16 cm) and dried in a vacuum oven overnight. All the dried films were preconditioned at 50 ± 5% RH for 48 h before analysis.

Figure.5 Fabrication of CD-AgNP/CNW- SPI polymer films for packaging

4.3 Characterization of nanoparticles and composite films

Morphological analysis of the nanoparticles was done using a Transmission Electron microscope (TEM). The absorbance of CD and AgNP was measured using UV-Visible double beam spectrometer model in the scan range 190-900 nm.

Fluorescence spectra of CD and AgNP were analysed using a PL spectrophotometer operated at 280-450 nm range of excitation wavelengths. The surface morphology of SPI biocomposite films was observed using SEM (Secondary Electron Microscope) operating at an accelerating voltage of 20 kV.

XRD of CNW and SPI composite films was done using Siemens X-ray diffractometer D5000 instrument using Ni-filtered Cu Kα radiation operating at 40 kV and 30 mA. The degree of crystallinity of CNW was calculated using Segal Equation [49]. The crystal size of CNW was calculated using the Scherrer equation [50].

Functional groups in CNW and SPI composites were observed using FTIR spectroscopy in the scan range of 4000-500 cm^{-1} and resolution 4 cm^{-1}.

Water vapor permeability of the films were determined by, film sample (7 cm x 7 cm) was mounted on a cup (6.8 cm diameter and 2.5 cm depth) containing 18 mL distilled water and sealed. The cups were placed in a humidity chamber maintained at 25 °C and 50% RH and the weight changes of the cups were measured at 1 h interval for 8 h. The WVP (g.m/m^{-2}.Pa.s) of the film was calculated as

$$WVP=\frac{WxX}{txAx\Delta P}$$

where W = increased weight of test vessel (g), x = thickness (m), t = time (s) for weight change of the cup, A= film permeation area (m^2), and ΔP is the partial water vapor pressure difference across two sides of the film.

Soil biodegradation analysis, the samples were cut into (2 cm x 2 cm), dried in an air oven at 105ºC for 24 h and weighed (W1). The films were then buried in plastic boxes at a depth of 10 cm from the soil to ensure aerobic degradation. The analysis was done at 32 ºC at a relative humidity of 35% by adding water periodically. The excess water was drained off through a hole at the bottom of the box. After

stipulated period, the samples were taken out from the soil, washed gently to wipe out the soil particles and dried in the oven at 105ºC for a period of 12 h and weighed (W2). The extend of degradation was measured in terms of % weight loss using the following

$$\text{WL (\%)} = \frac{W1 - W2}{W1} \; x \; 100$$

CHAPTER 5

RESULT AND DISCUSSION

5.1 Characterization of Nanoparticles

5.1.1 Characterization of AgNP

In this work, SPI has been used as a precursor to produce the CD. The surface of CD produced from SPI will be covered with functional groups such as -OH, $-NH_2$ etc., which can donate electrons to Ag^+ and reduce it to Ag (0). In this process, CD acts as a template to which Ag(0) can anchor. On mixing $AgNO_3$ with CD, a yellow solution was formed which when placed under UV turned brown within minutes.

The colour change indicated the complete nucleation and growth of AgNP on CD. HRTEM image (**Figure 5**) shows that each synthesized AgNP is anchored on each CD. Size histogram shows that most of the AgNP are in the range of 12-14 nm in size. The absorbance peak of CD and the synthesized AgNP are shown in (**Figure 5)**. CD shows a strong absorption at 206 nm due to the π-π* transition of aromatic C = C bonds. A small hump at 260 nm is attributed to the n-π* transition of C=O bonds[08] . The UV-Visible spectra of AgNP show an absorption band at 482 nm attributed to surface plasmon absorption of AgNP. However, the fluorescence of CD was completely quenched by adding $AgNO_3$ solution (**Figure 5(B))**. Since AgNP is formed by utilizing the reducing property of AgNP, electrons transfer from CD to Ag (I) takes place, resulting in the quenching of fluorescence . It is observed that no colour change or agglomeration happened for the colloidal solution of AgNP even after storage for 30 days. This indicates that CD can serve as a stabilizing agent for AgNP and prevent its aggregation.

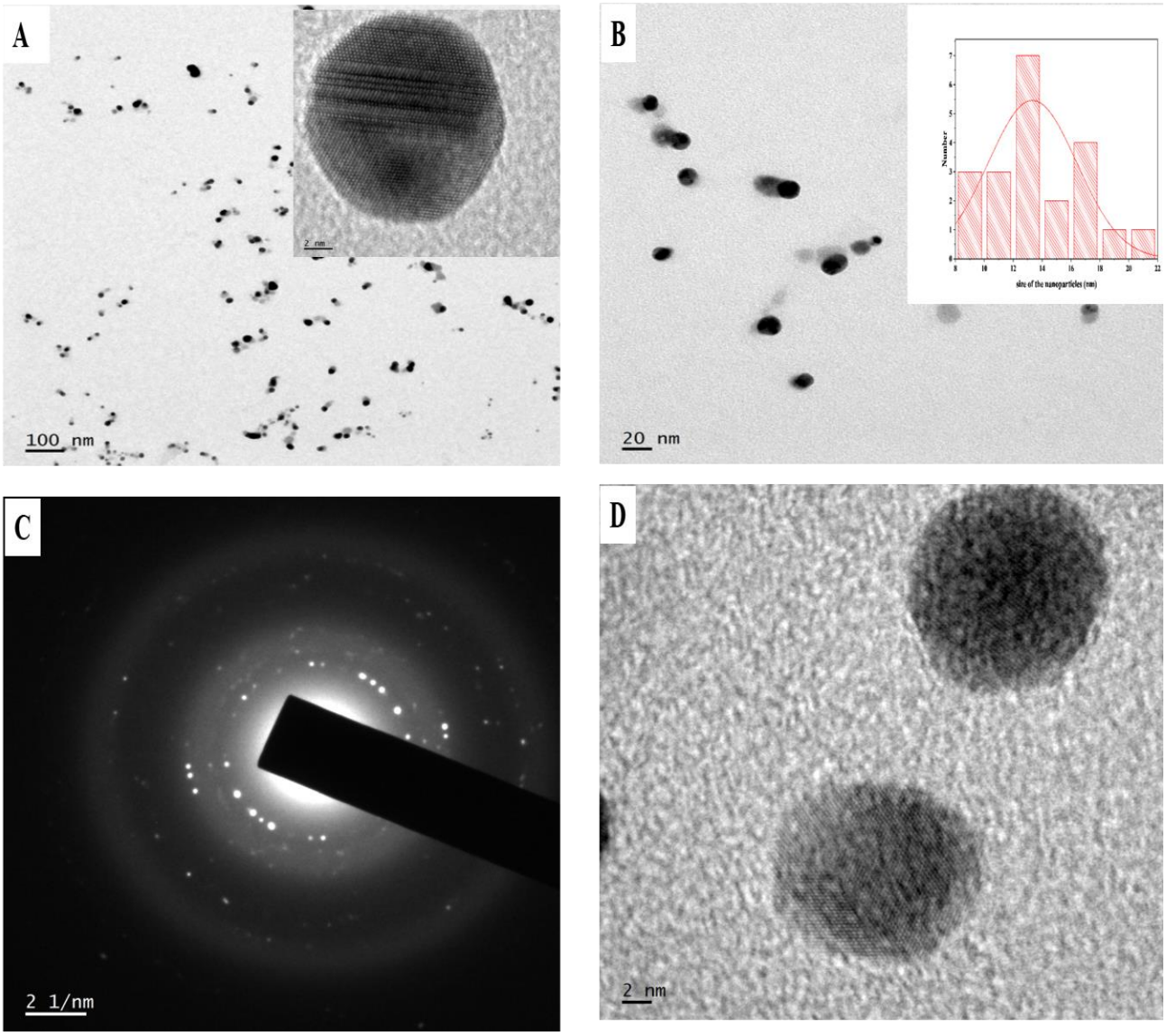

Figure 6: TEM and HRTEM images of AgNP. The inset image in (B) shows the size distribution histogram with a Gaussian fitting curve.

5.1.2 Characterization of CNW

TEM images of CNW are shown in **Figure 6(A)**. These reveal that CNW suspension consists of aggregated and individual nanocrystals. The individual crystals had a needle-like morphology with a wide range of length distribution ranging from 100 to 400 nm. The XRD pattern of CNW is shown in **Figure 6(B)**. The diffractogram shows typical peaks at 2θ values 19º, 9º, 23º corresponding to highly crystalline CNW. The absence of diffraction peak at 29.6º shows the complete removal of calcium carbonate during the demineralization step. The presence of well-defined diffraction peaks proves the existence of

crystalline CNW with a crystallinity index value of 99.67 %. The crystal size calculated from the Scherrer equation was between 5 nm and 9 nm. The UV absorption spectra of CNW (**Figure 6(C)**) shows a maximum absorption band at 194 nm owing to the presence of chromophoric groups glucosamine and N-acetyl glucosamine. The absence of absorption band at 280 nm due to aromatic amino acid groups shows that complete protein removal occurred during the deproteinization step. The FTIR spectrum of CNW is given in **Figure 6(D)**. The characteristic absorption band of CNW such as OH stretching band at 3372 cm^{-1}, NH stretching band at 3259 cm^{-1}, CH_3 and CH_2 stretching band at 2877 cm^{-1}, amide I band at 1649 and 1626 cm^{-1}, amide II at 1556 cm^{-1}, methyl CH stretch at 1379 cm^{-1} and 1313 cm^{-1} and amide III bands at 1243 cm^{-1}, were observed . The peak at 1153 cm^{-1} corresponds to glycosidic C-O-C stretching. Strong peaks at 1022 and 1070 cm^{-1} are attributed to the saccharide structure present in the carbohydrate backbone. A peak at 935 cm^{-1}corresponds to the β-linkage of the glucopyranose ring of chitin.

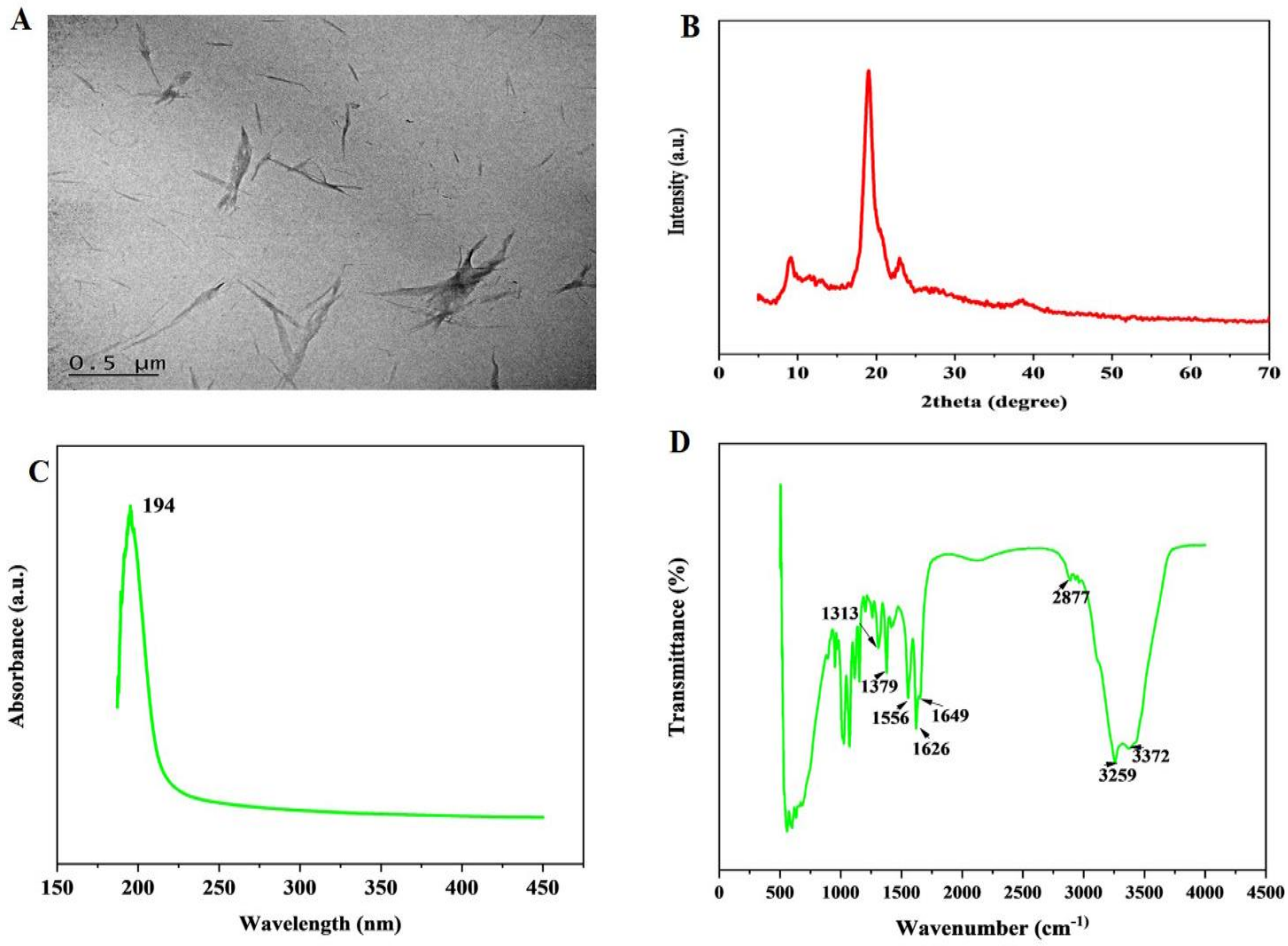

Figure 7:(A) TEM images of CNW, (B) XRD spectra of CNW, (C) UV-Visible absorption spectra of CNW, (D) FTIR spectra of CNW.

5.2 Characterization of the Nanocomposite films

5.2.1 SEM

Figure 8 shows the SEM micrographs of SPI, SPI-CNW, SPI-AgNP and SPI-CNW-AgNP composite films. Pure SPI film exhibited a homogenous and smooth surface without any pores or cracks, providing evidence of the high film-forming property of SPI. The incorporation of CNW (**Figure 8(B)**) in the SPI matrix made the surface compact and rough, indicating the interaction between SPI and CNW. similar morphological changes when diatomite was incorporated into the SPI matrix. In the SPI films with AgNP (**Figure 8(C)**), flower-like AgNP was found to be uniformly distributed in the SPI matrix. Compared to SPI-CNW and SPI-AgNP film, SPI-CNW-AgNP film exhibited a unique surface morphology without any visible aggregation of CNW or AgNP (**Figure 8(D)**).

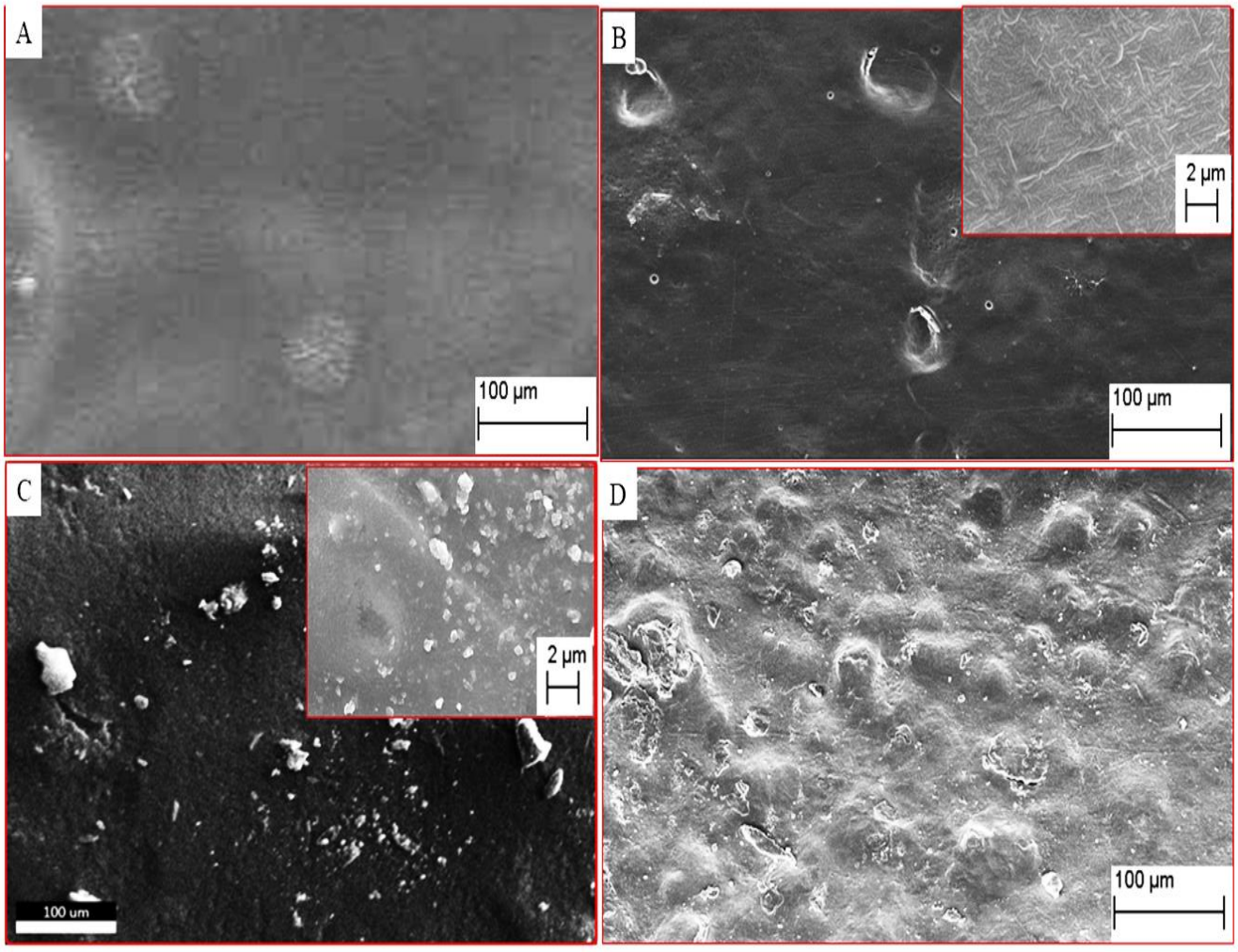

Figure 8: SEM micrographs of (A) SPI, (B) SPI-8CNW, (C) SPI-AgNP (D) SPI-CNW-AgNP films

5.2.2 FTIR Analysis

FTIR spectrum of SPI, SPI-CNW, SPI-AgNP and SPI-CNW-AgNP composites are shown in **Figure 9 (A)**. The control SPI contains characteristic bands at 3100-3500 cm^{-1} attributed to free and bound OH and NH stretching vibrations, 2929 cm^{-1} assigned to CH asymmetric stretching vibrations, 1631 cm^{-1} assigned to amide I band due to C=O stretching vibrations,1537 cm^{-1} attributed to amide II band corresponding to NH bending and CH deformation, 1398 cm^{-1} corresponding to CH_3 deformation and 1235 cm^{-1} attributed to amide III band corresponding to NH bending and CN stretching. Peaks below 1200 cm^{-1} correspond to the fingerprint region. As both SPI and CNW contain the same amide and amino groups, the FTIR spectrum of the two shows similarity in the spectrum. Only slight changes in peak positions and intensity could be observed. The intensity of peak around 3268 cm^{-1} increased with increasing concentration of CNW showing hydrogen bond formation between SPI and CNW . A slight shift in the amide I and amide II band show that changes have occurred in the secondary structure of protein on the addition of fillers which reveals that interactions have occurred between SPI and the fillers. Due to the very low concentration of AgNP, not much change in band intensity or position could be observed on the addition of AgNP. However, it has been reported that the acetamide and hydroxyl groups present in the structure of CNW will favour the attachment of AgNP onto its surface thus stabilizing Ag(0) nanoparticles.

5.2.3 XRD Analysis

XRD patterns of SPI, SPI-CNW, SPI-AgNP and SPI-CNW-AgNP composites are shown in **Figure 9(B)**. The control SPI film has weak characteristic peaks at 10.2º and 22º, which show the low degree of crystallinity of the SPI matrix. At a lower concentration of CNW (< 4%) similar peaks were obtained for SPI and SPI-CNW, suggesting that the ordered structure of SPI was kept even after CNW addition, glycerol-plasticizing and solvent casting. This indicates that when a low concentration of CNW was added into the SPI matrix, it was dispersed homogeneously into the amorphous domains of the SPI matrix, maintaining the ordered structure of the SPI matrix. However, while the CNW content increased to 10 wt%, the peak at 22º and 10.2º shifted to 19º and 9º typically assigned to CNW. Increasing CNW content induces the self-aggregation of CNW, resulting in the size expansion of aggregated CNW domains. This results in the partial destruction of the ordered structure of SPI. XRD of AgNP is reported to possess characteristic peaks at 36.2º, 43º, 63.6º and 76º. However, all the said peaks disappeared in SPI-AgNP nanocomposites. The peak intensity and position of pure SPI did not change in the presence

of AgNP. This proves that AgNP is uniformly distributed in the SPI matrix and has good interaction with the matrix. In SPI-CNW-AgNP composites, the crystallinity of CNW was retained proving that CNW is more crystalline than AgNP thereby increasing the overall crystallinity of the composites .

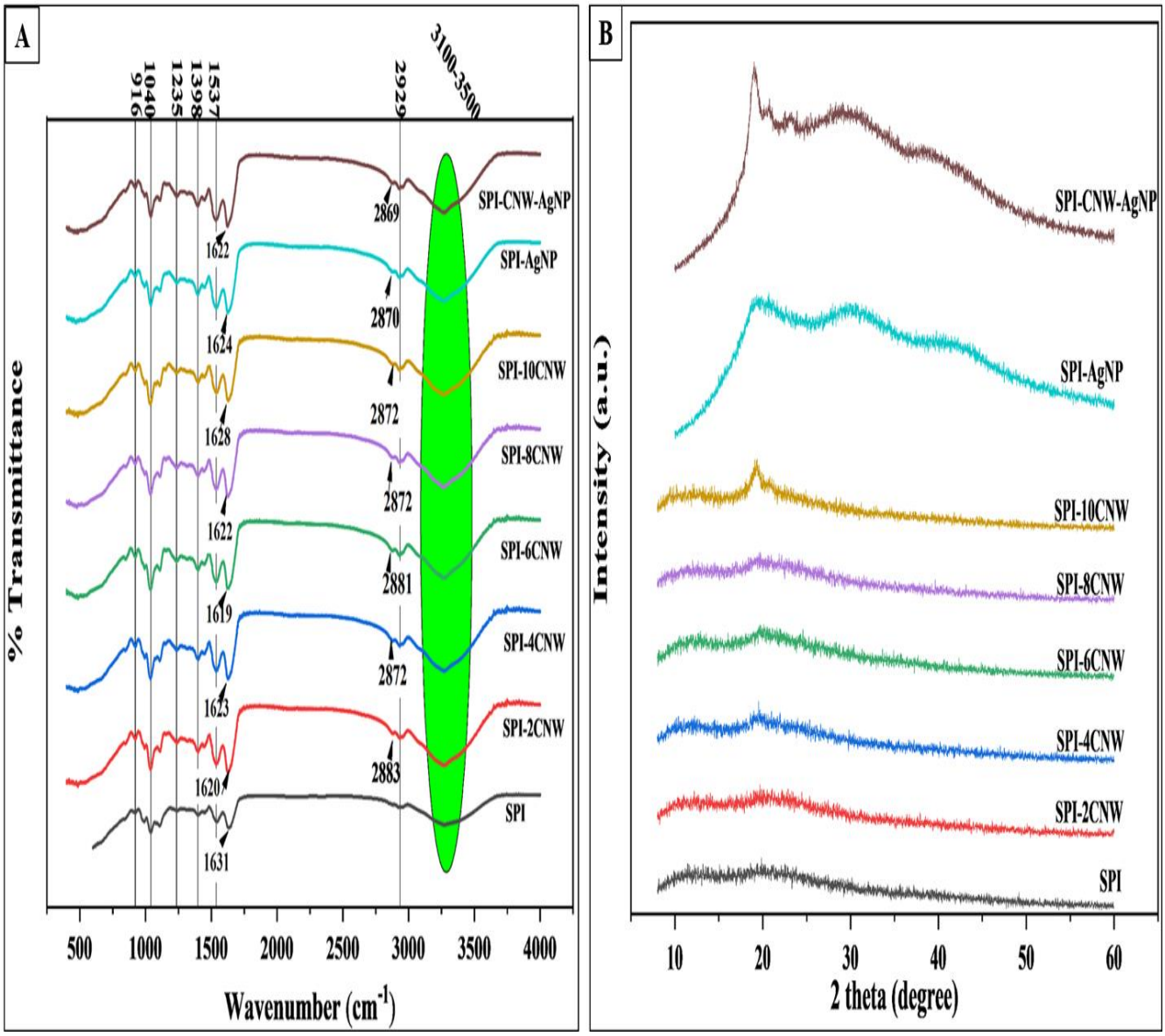

Figure 9: (A) FTIR and (B) XRD of SPI and SPI composites

5.2.4 **Water Vapour Permeability**

The decrease in WVP is an important criterion which determines the applicability of biopolymer films for use in food coatings, packaging etc. The WVP of SPI and SPI nanocomposite films are shown in Table. The WVP value of control SPI film was (2.75±0.16) x 10^{-9}g.m/m^2.Pa.s, which decreased significantly ($p<0.05$) on addition of CNW/AgNP. The lowest values (0.87±0.33) and (0.54±0.31) were obtained for SPI-6CNW and SPI-CNW-AgNP nanocomposite films. The decrease in WVP can be attributed to the homogenous distribution of nanoparticle in the polymer matrix which offers a torturous pathway for the water vapour while travelling through the film thereby increasing the path length for diffusion. The WVP values for SPI films with higher CNW concentrations (>6%) was slightly higher due to slight aggregation of CNW in SPI matrix which actually decreased the presence of CNW in some parts of the matrix thereby facilitating the permeability of water vapour through the matrix. However, on addition of both AgNP to 8%CNW, the combined reinforcement of both the nanoparticles led to a further decrease in WVP.

Films	WVP (10^{-9}g.m/m^2.Pa.s)
SPI	2.75 ± 0.16^{a}
SPI-2CNW	2.48 ± 0.49^{ab}
SPI-4CNW	2.01 ± 0.11^{b}
SPI-6CNW	0.87 ± 0.33^{de}
SPI-8CNW	1.02 ± 0.16^{de}
SPI-10CNW	1.44 ± 0.42^{cd}
SPI-AgNP	1.94 ± 0.28^{bc}
SPI-CNW-AgNP	0.54 ± 0.31^{e}

5.2.5. Biodegradability test

Biodegradability is an important parameter that should be measured in the case of packaging films. **Figure 10** shows the effect of AgNP/ CNW on the biodegradability rate of SPI nanocomposite films. It is observed that the biodegradability rate of pure SPI films increased upto 90% with the increase in burial time. However, the rate of biodegradability of nanocomposite film was slightly less than the control film. When CNW/AgNP was added to the SPI film, because of the strong interactions happening between SPI and the nanofillers, the degradation becomes difficult due to greater difficulty in breaking the bond between the matrix and the fillers [51]. The lowest degradation rate was observed for SPI-CNW-AgNP film which indirectly hints the strong association of the two fillers with the matrix.

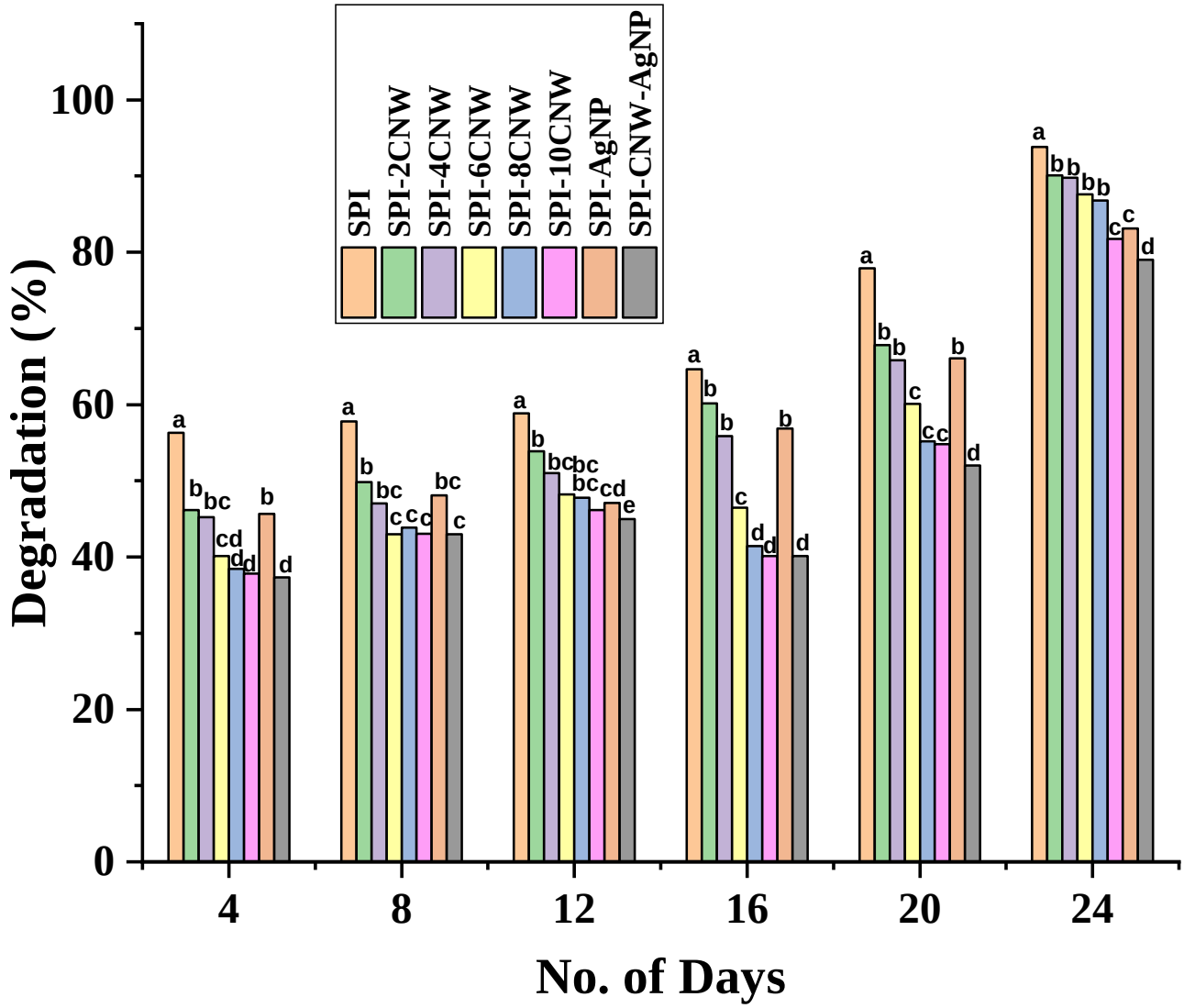

Figure 10: Biodegradation analysis of the films

CHAPTER 6

CONCLUSION

In summary, AgNP and CNW were used to produce active SPI based nanocomposite films with improved properties. AgNP was synthesized using the reducing and capping ability of the carbon dot solution. The water vapour permeability studies, and biodegradability of the films supports its properties and proposed application. Thus SPI-CNW-AgNP nanocomposite film has immense potential for commercial application as active food packaging material. Further studies can focus on the specific interactions of the nanoparticles with the different kinds of food materials packed using the SPI film. The synthesis strategy provides new insights to design and fabricate high-performance SPI-based nanocomposite.

CHAPTER 7

REFERENCES

1. Rajkovic, A., Smigic, N., & Devlieghere, F. (2010). Contemporary strategies in combating microbial contamination in food chain. International Journal of Food Microbiology, 141, S29-S42.
2. Thakali, A., & MacRae, J. D. (2021). A review of chemical and microbial contamination in food: What are the threats to a circular food system?. Environmental Research, 194, 110635.
3. Fu, Y., & Dudley, E. G. (2021). Antimicrobial-coated films as food packaging: A review. Comprehensive Reviews in Food Science and Food Safety, 20(4), 3404-3437.
4. Pereira, P. F., de Sousa Picciani, P. H., Calado, V., & Tonon, R. V. (2021). Electrical gas sensors for meat freshness assessment and quality monitoring: A review. Trends in Food Science & Technology, 118, 36-44.
5. Subramanian, K., Logaraj, H., Ramesh, V., Mani, M., Balakrishnan, K., Selvaraj, H., ... & Aruni, W. (2022). Intelligent pH Indicative Film from Plant-Based Extract for Active Biodegradable Smart Food Packing. Journal of Nanomaterials, 2022.
6. Fang, Z., Zhao, Y., Warner, R. D., & Johnson, S. K. (2017). Active and intelligent packaging in meat industry. *Trends in Food Science & Technology*, *61*, 60-71.
7. Janjarasskul, T., & Suppakul, P. (2018). Active and intelligent packaging: The indication of quality and safety. Critical reviews in food science and nutrition, 58(5), 808-831.
8. Biji, K. B., Ravishankar, C. N., Mohan, C. O., & Srinivasa Gopal, T. K. (2015). Smart packaging systems for food applications: a review. Journal of food science and technology, 52(10), 6125-6135.
9. Koshy, R. R., Mary, S. K., Thomas, S., & Pothan, L. A. (2015). Environment friendly green composites based on soy protein isolate–A review. Food Hydrocolloids, 50, 174-192.

10. Gowthaman, N. S. K., Lim, H. N., Sreeraj, T. R., Amalraj, A., & Gopi, S. (2021). Advantages of biopolymers over synthetic polymers: social, economic, and environmental aspects. In Biopolymers and their Industrial Applications (pp. 351-372). Elsevier.
11. Mincea, M., Negrulescu, A., & Ostafe, V. (2012). Preparation, modification, and applications of chitin nanowhiskers: a review. Rev. Adv. Mater. Sci, 30(3), 225-242.
12. Andrade, P. F., de Faria, A. F., Oliveira, S. R., Arruda, M. A. Z., & do Carmo Gonçalves, M. (2015). Improved antibacterial activity of nanofiltration polysulfone membranes modified with silver nanoparticles. Water Research, 81, 333-342.
13. Shen, L., Chen, M., Hu, L., Chen, X., & Wang, J. (2013). Growth and stabilization of silver nanoparticles on carbon dots and sensing application. Langmuir, 29(52), 16135-16140.
14. Gleiter, H. (2000). Nanostructured materials: basic concepts and microstructure. Acta materialia, 48(1), 1-29.
15. Kumar, R. (2013). Blends of polylactic acid and arylated soy protein isolate with triacetine as plasticiser. Plastics, rubber and composites, 42(7), 308-314.
16. Vieira, M. G. A., da Silva, M. A., dos Santos, L. O., & Beppu, M. M. (2011). Natural-based plasticizers and biopolymer films: A review. European polymer journal, 47(3), 254-263.
17. Tang, C. H. (2017). Emulsifying properties of soy proteins: A critical review with emphasis on the role of conformational flexibility. Critical Reviews in Food Science and Nutrition, 57(12), 2636-2679.
18. Bajpai, S. K., Chand, N., Ahuja, S., & Roy, M. K. (2015). Vapor induced phase inversion technique to prepare chitosan/microcrystalline cellulose composite films: Synthesis, characterization and moisture absorption study. Cellulose, 22(6), 3825-3837.
19. Atchudan, R., Jebakumar Immanuel Edison, T. N., Perumal, S., & Lee, Y. R. (2018). Indian gooseberry-derived tunable fluorescent carbon dots as a promise for in vitro/in vivo multicolor bioimaging and fluorescent ink. Acs Omega, 3(12), 17590-17601.

20. Singh, S. P., Bhargava, C. S., Dubey, V., Mishra, A., & Singh, Y. (2017). Silver nanoparticles: Biomedical applications, toxicity, and safety issues. International Journal of Research in Pharmacy and Pharmaceutical Sciences, 4(2), 1-10.
21. Mincea, M., Negrulescu, A., & Ostafe, V. (2012). Preparation, modification, and applications of chitin nanowhiskers: a review. Rev. Adv. Mater. Sci, 30(3), 225-242.
22. Wang, D., Wang, Z., Zhan, Q., Pu, Y., Wang, J. X., Foster, N. R., & Dai, L. (2017). Facile and scalable preparation of fluorescent carbon dots for multifunctional applications. Engineering, 3(3), 402-408.
23. Ding, H., Yu, S. B., Wei, J. S., & Xiong, H. M. (2016). Full-color light-emitting carbon dots with a surface-state-controlled luminescence mechanism. ACS nano, 10(1), 484-491.
24. De Jong, W. H. (2008). Borm pJ. Drug delivery and nanoparticles: applications and hazards. Int J Nanomedicine, 3, 133-149.
25. Guo, S., Li, H., Liu, J., Yang, Y., Kong, W., Qiao, S., ... & Kang, Z. (2015). Visible-light-induced effects of Au nanoparticle on laccase catalytic activity. ACS applied materials & interfaces, 7(37), 20937-20944.
26. Canevari, T. C., Nakamura, M., Cincotto, F. H., de Melo, F. M., & Toma, H. E. (2016). High performance electrochemical sensors for dopamine and epinephrine using nanocrystalline carbon quantum dots obtained under controlled chronoamperometric conditions. Electrochimica Acta, 209, 464-470.
27. Saud, P. S., Pant, B., Alam, A. M., Ghouri, Z. K., Park, M., & Kim, H. Y. (2015). Carbon quantum dots anchored TiO2 nanofibers: Effective photocatalyst for waste water treatment. Ceramics International, 41(9), 11953-11959.

28. Zhang, F., Feng, X., Zhang, Y., Yan, L., Yang, Y., & Liu, X. (2016). Photoluminescent carbon quantum dots as a directly film-forming phosphor towards white LEDs. Nanoscale, 8(16), 8618-8632.
29. Bottini, M., Balasubramanian, C., Dawson, M. I., Bergamaschi, A., Bellucci, S., & Mustelin, T. (2006). Isolation and characterization of fluorescent nanoparticles from pristine and oxidized electric arc-produced single-walled carbon nanotubes. The Journal of Physical Chemistry B, 110(2), 831-836.
30. Hu, S., Guo, Y., & Tian, R. (2011, July). Synthesis and size control of carbon quantum dots by tailoring laser parameters. In Proceedings of 2011 International Conference on Electronics and Optoelectronics (Vol. 2, pp. V2-283). IEEE.
31. Yao, S., Hu, Y., & Li, G. (2014). A one-step sonoelectrochemical preparation method of pure blue fluorescent carbon nanoparticles under a high intensity electric field. Carbon, 66, 77-83.
32. Zhang, F., Feng, X., Zhang, Y., Yan, L., Yang, Y., & Liu, X. (2016). Photoluminescent carbon quantum dots as a directly film-forming phosphor towards white LEDs. Nanoscale, 8(16), 8618-8632.
33. Zuo, P., Xiao, D., Gao, M., Peng, J., Pan, R., Xia, Y., & He, H. (2014). Single-step preparation of fluorescent carbon nanoparticles, and their application as a fluorometric probe for quercetin. Microchimica Acta, 181(11), 1309-1316.
34. Luo, Z., Qi, G., Chen, K., Zou, M., Yuwen, L., Zhang, X., ... & Wang, L. (2016). Microwave-assisted preparation of white fluorescent graphene quantum dots as a novel phosphor for enhanced white-light-emitting diodes. Advanced Functional Materials, 26(16), 2739-2744.

35. Shi, H., Wei, J., Qiang, L., Chen, X., & Meng, X. (2014). Fluorescent carbon dots for bioimaging and biosensing applications. Journal of biomedical nanotechnology, 10(10), 2677-2699.
36. Siddique, A. B., Singh, V. P., Pramanick, A. K., & Ray, M. (2020). Amorphous carbon dot and chitosan based composites as fluorescent inks and luminescent films. Materials Chemistry and Physics, 249, 122984.
37. Fang, L., Xu, Q., Zheng, X., Zhang, W., Zheng, J., Wu, M., & Wu, W. (2016). Soy flour-derived carbon dots: facile preparation, fluorescence enhancement, and sensitive Fe3+ detection. Journal of Nanoparticle Research, 18(8), 1-13.
38. Jana, J., Gauri, S. S., Ganguly, M., Dey, S., & Pal, T. (2015). Silver nanoparticle anchored carbon dots for improved sensing, catalytic and intriguing antimicrobial activity. Dalton Transactions, 44(47), 20692-20707.
39. Zhai, X., Shi, J., Zou, X., Wang, S., Jiang, C., Zhang, J., ... & Holmes, M. (2017). Novel colorimetric films based on starch/polyvinyl alcohol incorporated with roselle anthocyanins for fish freshness monitoring. Food Hydrocolloids, 69, 308-317.
40. Aurlina, R., Gopi, R. R., Ebenezer, T., Prabu, H. J., & Johnson, I. (2022). Antibacterial study of silver nanoparticles synthesized using Strychnos potatorum (linn)–Green synthesis method. Materials Today: Proceedings.
41. Rani, S., Kumar, K. D., Mandal, S., & Kumar, R. (2020). Functionalized carbon dot nanoparticles reinforced soy protein isolate biopolymeric film. Journal of Polymer Research, 27(10), 1-10.

42. Kumar, R., Anjum, K. N., Rani, S., Sharma, K., Tiwary, K. P., & Kumar, K. D. (2019). Material properties of ZnS nanoparticles incorporated soy protein isolate biopolymeric film. Plastics, Rubber and Composites, 48(10), 448-455.
43. Rani, S., Singh, A. K., Paswan, R. R., Kumar, K. D., & Kumar, R. (2020). Preparation, characterization and antibacterial evaluation of soy protein isolate biopolymeric films loaded with nalidixic acid. Journal of Polymers and the Environment, 28(7), 1841-1850.
44. Liu, T., Liu, Z., Zhang, J., Shi, S. Q., Gong, S., & Li, J. (2022). An ultrastrong bioinspired soy protein isolate-based nanocomposite with graphene oxide intercalation. Composites Part B: Engineering, 236, 109805.
45. Yoshida, C. M., Maciel, V. B. V., Mendonça, M. E. D., & Franco, T. T. (2014). Chitosan biobased and intelligent films: Monitoring pH variations. LWT-food science and technology, 55(1), 83-89.
46. Yan, Y., Wang, K., Wang, Z., Gindl-Altmutter, W., Zhang, S., & Li, J. (2017). Fabrication of homogeneous and enhanced soybean protein isolate-based composite films via incorporating TEMPO oxidized nanofibrillated cellulose stablized nano-ZnO hybrid. Cellulose, 24(11), 4807-4819.
47. Fan, Y., Saito, T., & Isogai, A. (2008). Preparation of chitin nanofibers from squid pen β-chitin by simple mechanical treatment under acid conditions. Biomacromolecules, 9(7), 1919-1923.
48. Jafari, H., Pirouzifard, M., Khaledabad, M. A., & Almasi, H. (2016). Effect of chitin nanofiber on the morphological and physical properties of chitosan/silver nanoparticle bionanocomposite films. International journal of biological macromolecules, 92, 461-466.

49. Segal, L. G. J. M. A., Creely, J. J., Martin Jr, A. E., & Conrad, C. M. (1959). An empirical method for estimating the degree of crystallinity of native cellulose using the X-ray diffractometer. Textile research journal, 29(10), 786-794.
50. Shankar, S., & Rhim, J. W. (2016). Tocopherol-mediated synthesis of silver nanoparticles and preparation of antimicrobial PBAT/silver nanoparticles composite films. LWT-Food Science and Technology, 72, 149-156.
51. Deepa, B., Abraham, E., Pothan, L. A., Cordeiro, N., Faria, M., & Thomas, S. (2016). Biodegradable nanocomposite films based on sodium alginate and cellulose nanofibrils. Materials, 9(1), 50.